Dirichlet-to-Neumann Mapping Method for Bandgap Analysis in 2D Superconducting Photonic Crystals

Kaiye Chen [1, 2, a], Jianhua Yuan [1, 2, b, *]

[1] School of Mathematical Sciences, Beijing University of Posts and Telecommunications, Beijing 100876, China;

[2] Key Laboratory of Mathematics and Information Networks (Beijing University of Posts and Telecommunications), Ministry of Education, Beijing 100876, China.

[a] chenkaiye@bupt.edu.cn, [b] jianhuayuan@bupt.edu.cn

Abstract. This study employs the Dirichlet-to-Neumann (DtN) method to analyze superconducting photonic crystals (SPCs). By building a DtN operator for the unit cell lattice, we develop an eigenvalue framework to calculate photonic bandgap structures in niobium (Nb) and yttrium barium copper oxide (YBCO) SPCs. This boundary-only discretization approach (avoiding full structural meshing) enhances computational efficiency. We systematically analyze temperature effects on bandgap properties and cutoff frequencies below YBCO's critical temperature. Results of numerical experiments confirm the DtN method's reliability and efficiency for studying SPC bandgap characteristics.

Keywords: superconducting photonic crystals; photonic bandgap; Dirichlet-to-Neumann map; numerical methods.

1. Introduction

Photonic crystals (PCs) are artificial periodic optical materials with unique photonic bandgap (PBG) structures, analogous to semiconductor electronic states, enabling advanced light manipulation for optoelectronic applications. Following Yablonovitch and John's foundational work [1,2], PBG properties have been extensively utilized in designing photonic crystal devices, such as waveguides[3], frequency filters[4], and ultrahigh-Q components [5,6].Recent research has expanded to unconventional materials like dispersive superconducting photonic crystals (SPCs) [7-9]. Unlike conventional PCs, superconducting materials exhibit frequency-, temperature-, and magnetic field-dependent refractive indices, enabling dynamic PBG tuning.

For 2D-SPCs, key challenges involve developing efficient numerical methods to compute PBG structures. Traditional approaches (PWE) [10], FEM [11-12], FDTD [13]) struggle with material limitations and nonlinear dispersive effects. Current superconducting PBG calculations rely on modified methods (Band structure-transmission optimization-band structure method [14],improved PWE [15], TMM [16], FEM [17],). Notably, the DtN mapping method by Yuan, Hu et al. [18-20] revolutionized this field by discretizing only unit lattice boundaries via field-normal derivative mapping, drastically reducing computational complexity.

For this study, we apply the DtN method to analyze 2D-SPC bandgap structures, extending numerical frameworks for such systems. We further systematically examine how superconducting material filling ratios and ambient temperatures influence PBG properties.

2. Model and algorithm

2.1 Superconducting photonic crystal

2.1.1 Superconducting material

Superconducting materials are quantum materials exhibiting zero electrical resistance and perfect diamagnetism below the critical temperature (T_c) [21].The investigated two-dimensional superconducting photonic crystals consist of periodically arranged cylindrical rods made of

superconducting material, embedded in a surrounding material with a refractive index n_2 = 1.0. The primary superconducting materials studied here are low-temperature superconductor niobium (Nb) and high-temperature superconductor (YBCO).

In this work, the refractive index n_1 of superconducting materials (Nb and YBCO) in cylindrical configurations can be expressed under the non-magnetic material assumption as:

$$n_1(\omega,T)=\sqrt{\varepsilon_1(\omega,T)}. \tag{1}$$

Key parameters include the angular frequency (ω), temperature (T), and the superconducting material's dielectric constant (ε_1).Below the critical temperature T_c, Ref. [14,15] shows that neglecting normal electron contributions, the dielectric response is given by the classical two-fluid model and London local dynamic model as:

$$\varepsilon_1=1-\frac{1}{\omega^2\varepsilon_0\mu_0{\lambda_L}^2}=1-\frac{\mathrm{c}^2}{\omega^2{\lambda_L}^2} \quad \text{where ,}\ c=\frac{1}{\sqrt{\varepsilon_0\mu_0}}. \tag{2}$$

Here, μ_0 denotes the vacuum permeability, ε_0 the vacuum permittivity, and c the velocity of light. Additionally, λ_L represents the London penetration depth, which is temperature-dependent and will be expressed below.(The penetration depth extrapolated to T = 0K is λ_0 .)

$$\lambda_L=\lambda_L(T)=\frac{\lambda_0}{\sqrt{1-(\frac{T}{T_c})^4}}. \tag{3}$$

2.1.2 Control equations

For 2D PCs, under E-polarization, our governing equations are the following Helmholtz equations, derived from the set of Maxwell's equations [18,19]:

$$\frac{\partial^2 u}{\partial x^2}+\frac{\partial^2 u}{\partial y^2}+{k_0}^2n^2u=0 \tag{4}$$

For model simplification, this study exclusively considers E-polarized cases. In Equation (4), u represents the z-axis electric field component, with k_0 denoting the free-space wavenumber and n the refractive index of the photonic crystal material. Since the cylindrical medium is a superconducting medium, its refractive index depends not only on the position but also on the frequency ω and temperature T. Therefore, the refractive index n will be expressed as: $n=n(x,y,\omega,T)$ .Assume that the cylindrical radius is a,the lattice constant of is L, and b_1 and b_2 are arbitrary integers. n satisfies the periodic condition: $n(x,y,\omega,T)=n(x+b_1L,y+b_2L,\omega,T)$.

Assuming the cylinder is centered within the unit cell and embedded in a homogeneous medium, for the unit cell defined by $(x, y)\in[0, L]\times[0, L]$, we have:

$$n(x,y,\omega,T)=\begin{cases}n_1(\omega,T), r\le a\\ n2, r>a\end{cases}. \tag{5}$$

Here, n_1 and n_2 denote the refractive indices of the superconducting material within the cylinder and the surrounding medium. The polar coordinates (r,θ) are defined such that r = 0 corresponds to the lattice center at $x = y = L/2$.

2.2 Dirichlet-to-Neumann Mapping.

To calculate the bandgap structure of 2D superconducting PCs, constructing the DtN mapping for their unit lattice is essential to formulate the eigenvalue problem. The DtN operator Λ maps the boundary values of the fluctuating field to its normal derivatives on the unit lattice boundary Γ_{all}, i.e.,

$$\Lambda u\,|_{\Gamma_{all}}=\frac{\partial u}{\partial v}|_{\Gamma_{all}}\ . \tag{6}$$

The boundary's unit normal vector is denoted by v. For the unit lattice of the square photonic crystal under our investigation, u_1, u_2, u_3, and u_4 are respectively the values of the field u on the edges $\Gamma_1, \Gamma_2, \Gamma_3$ and Γ_4 of the square unit lattice (as depicted in left of Fig. 1).

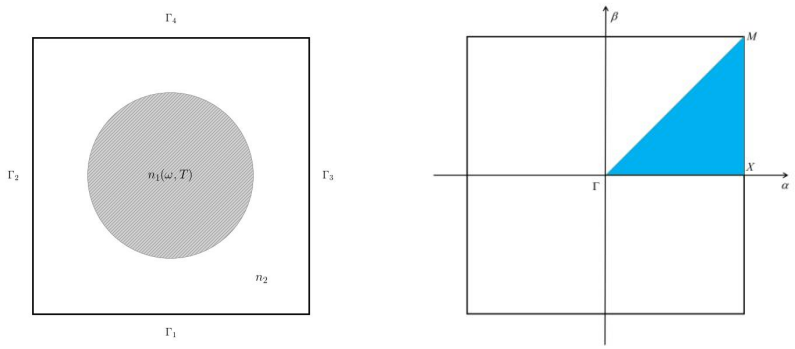

Fig. 1 Unit cell (left) and Brillouin zone (right)

From the definition of Λ it can be obtained that Λ satisfies the following equation:

$$\Lambda \begin{bmatrix} u_1 \\ u_2 \\ u_3 \\ u_4 \end{bmatrix} = \begin{bmatrix} \partial_y u_1 \\ \partial_x u_2 \\ \partial_x u_3 \\ \partial_y u_4 \end{bmatrix}. \tag{7}$$

Where, $u_1 = u(x,0)$, $u_2 = u(0,y)$, $u_3 = u(L,y)$, $u_4 = u(x,L)$ and $\partial_y u_1 = \partial_y u|_{y=0}$, $\partial_x u_2 = \partial_x u|_{x=0}$, $\partial_x u_{31} = \partial_x u|_{x=L}$, $\partial_y u_4 = \partial_y u|_{y=L}$.

Since in this paper we focus on the 2D square photonic crystal containing cylindrical dispersive medium, the general solution to Helmholtz equation (4) takes the form of a linear combination of particular solutions expressed via Bessel functions:

$$u(x,y) = \sum_{\mathrm{m}=-\infty}^{\infty} c_m \varphi_m(r) e^{im\theta} \qquad \text{where , } \varphi_m(r) = \begin{cases} J_{\mathrm{m}}(k_0 n_1(\omega,T) r) & , \ r \le \mathrm{a} \\ A_m J_{\mathrm{m}}(k_0 n_2 r) + B_m Y_m(k_0 n_2 r) & , \ r > \mathrm{a} \end{cases} \tag{8}$$

Applying the continuity of the field and its partial derivatives across $r = a$ allows solving for the coefficients A_m and B_m. Consequently, the normal derivative of $u(x, y)$ can also be represented by a linear combination of the particular solutions:

$$\frac{\partial u}{\partial v}(x,y) = \sum_{m=-\infty}^{m=+\infty} c_m \frac{\partial}{\partial v} \varphi_m(r) e^{im\theta}. \tag{9}$$

Subsequently, we carry out discretization treatment and adopt N discrete points on every side of the square lattice. The coordinates of these $4N$ discrete points are denoted as (x_k, y_k) , with corresponding polar coordinates (r_k, θ_k) , where k=1,2,⋯,$4N$.Therefore, equations (8) and (9) are discretized and truncated into:

$$u(x_k, y_k) = \sum_{\mathrm{m}=-2N}^{2N-1} c_m \varphi_m(r_k) e^{im\theta_k}, \tag{10}$$

$$\frac{\partial u}{\partial v}(x_k, y_k) = \sum_{m=-2N}^{2N-1} c_m \frac{\partial}{\partial v} \varphi_m(r_k) e^{im\theta_k}. \tag{11}$$

The corresponding matrix formulation is(P,Q are 4N*4N matrices.):

$$\vec{u} = P\vec{c} \ , \ \frac{\partial}{\partial v}\vec{u} = Q\vec{c} \ . \tag{12}$$

Here , $\vec{u} = [u(x_1, y_1), u(x_2, y_2), \cdots, u(x_{4N}, y_{4N})]^T$, $\vec{c} = [\mathrm{c}_{-2N}, \mathrm{c}_{-2N+1}, \cdots, \mathrm{c}_{2N-1}]^T$. Consequently, the approximate matrix for the DtN map is derived as $\Lambda = QP^{-1}$.

2.3 Eigenvalue problem.

To determine the bandgap properties of superconducting photonic crystals, we analyze Bloch-mode solutions to the Helmholtz equation (4):

$$u(x,y)=e^{i(\alpha x+\beta y)}\psi(x,y). \tag{13}$$

Where (α,β) denotes the bloch wave-vector.where $\psi(x,y)$ is a periodic function adhering to the same periodicity condition as the refractive index distribution $n(x,y,\omega,T)$ .For a two dimensional square lattice, the structural periodicity along the x- and y-directions imposes the following quasi-periodic boundary conditions:

$$\begin{aligned} u(x,L)&=\rho_\beta u(x,0), \quad \frac{\partial u(x,L)}{\partial y}=\rho_\beta \frac{\partial u(x,0)}{\partial y},\\ u(L,y)&=\rho_\alpha u(0,y), \quad \frac{\partial u(L,y)}{\partial x}=\rho_\alpha \frac{\partial u(0,y)}{\partial x}. \end{aligned} \tag{14}$$

Where $\rho_\alpha=e^{i\alpha L}$ and $\rho_\beta=e^{i\beta L}$. The matrix Λ is partitioned into a 4×4 block structure. Each block matrix is an $N\times N$ matrix. Hence, it follows from Equation (8) that:

$$\begin{pmatrix}\Lambda_{11}&\Lambda_{12}&\Lambda_{13}&\Lambda_{14}\\ \Lambda_{21}&\Lambda_{22}&\Lambda_{23}&\Lambda_{24}\\ \Lambda_{31}&\Lambda_{32}&\Lambda_{33}&\Lambda_{34}\\ \Lambda_{41}&\Lambda_{42}&\Lambda_{43}&\Lambda_{44}\end{pmatrix}\begin{pmatrix}u_1\\u_2\\u_3\\u_4\end{pmatrix}=\begin{pmatrix}\partial_y u_1\\ \partial_x u_2\\ \partial_x u_3\\ \partial_y u_4\end{pmatrix}. \tag{15}$$

The problem of solving bandgap structures in photonic crystals can be transformed into an eigenvalue problem based on the quasi-periodic conditions (14). As Yuan et al. [18,19] systematically demonstrated through their investigation, this problem can ultimately be formulated as a eigenvalue equation of the following form:

$$\lambda\begin{bmatrix}C_1&0\\0&I\end{bmatrix}V+\begin{bmatrix}C_2&C_3\\-I&0\end{bmatrix}V=0. \tag{16}$$

where $V=[\lambda U^T,U^T]$, $U=[u_1,u_2]^T$ .The parameters λ and the matrices C_1,C_2,C_3 are associated with the Brillouin zone of a two-dimensional square superconducting photonic crystal. The first Brillouin zone of this crystal is illustrated in Fig 1, where its irreducible Brillouin zone corresponds to the triangular region bounded by the vertices $\Gamma(\alpha=0,\beta=0)$, $X(\alpha=\pi/L,\beta=0)$ and $M(\alpha=\pi/L,\beta=\pi/L)$ (shown as the shaded area in Fig. 1).

The specific values of matrices C_1,C_2,and C_3 on the ΓX , XM , and $M\Gamma$ edges are as follows:

1. From point Γ to point X , $\beta=0$, $\lambda=e^{i\alpha L}$ $(0<\alpha\le\pi/L)$: we

$$C_1=\begin{bmatrix}0&0\\0&-\Lambda_{23}\end{bmatrix},C_2=\begin{bmatrix}0&\Lambda_{43}-\Lambda_{13}\\-\Lambda_{21}-\Lambda_{24}&\Lambda_{33}-\Lambda_{22}\end{bmatrix},C_3=\begin{bmatrix}\Lambda_{41}-\Lambda_{14}+\Lambda_{44}-\Lambda_{11}&\Lambda_{42}-\Lambda_{12}\\ \Lambda_{31}+\Lambda_{34}&\Lambda_{32}\end{bmatrix}. \tag{17}$$

2. From point X to point M , $\alpha=\pi/L$, $\lambda=e^{i\beta L}$ $(0<\beta\le\pi/L)$:

$$C_1=\begin{bmatrix}-\Lambda_{14}&0\\0&0\end{bmatrix},C_2=\begin{bmatrix}\Lambda_{44}-\Lambda_{11}&\Lambda_{13}-\Lambda_{12}\\ \Lambda_{34}+\Lambda_{24}&0\end{bmatrix},C_3=\begin{bmatrix}\Lambda_{41}&\Lambda_{42}-\Lambda_{43}\\ \Lambda_{31}+\Lambda_{21}&\Lambda_{32}-\Lambda_{23}+\Lambda_{22}-\Lambda_{33}\end{bmatrix}. \tag{18}$$

3. From point M to point Γ , $\lambda=e^{i\beta L}=e^{i\alpha L}$ $(0<\beta=\alpha\le\pi/L)$:

$$C_1=\begin{bmatrix}-\Lambda_{14}&-\Lambda_{13}\\-\Lambda_{24}&-\Lambda_{23}\end{bmatrix},C_2=\begin{bmatrix}\Lambda_{44}-\Lambda_{11}&\Lambda_{43}-\Lambda_{12}\\ \Lambda_{34}-\Lambda_{21}&\Lambda_{33}-\Lambda_{22}\end{bmatrix},C_3=\begin{bmatrix}\Lambda_{41}&\Lambda_{42}\\ \Lambda_{31}&\Lambda_{32}\end{bmatrix}. \tag{19}$$

Thus, by solving the eigenvalue problem through a linear eigenvalue numerical method, the bandgap structure of the superconducting photonic crystal was obtained.

3. Numerical examples

3.1 Bandgap structure

To verify the DtN method's effectiveness in analyzing superconducting photonic crystal bandgaps, we conducted numerical studies on a 2D square-lattice structure: niobium (Nb) cylindrical rods in air, previously analyzed by Arafa H. Aly et al. [15] using PWE. The parameters match their study: T_c = 9.2K, zero-temperature penetration depth λ_0 =83.4nm, operating temperature T = 4.2K, lattice constant L = 200nm, and rod radius a =0.5L. As shown in Fig. 2, our DtN-based calculations of bandgap structures and cutoff frequency(ω_c)-filling factor($f.f$) relationships align with Aly et al.'s numerical results [15], confirming method consistency.

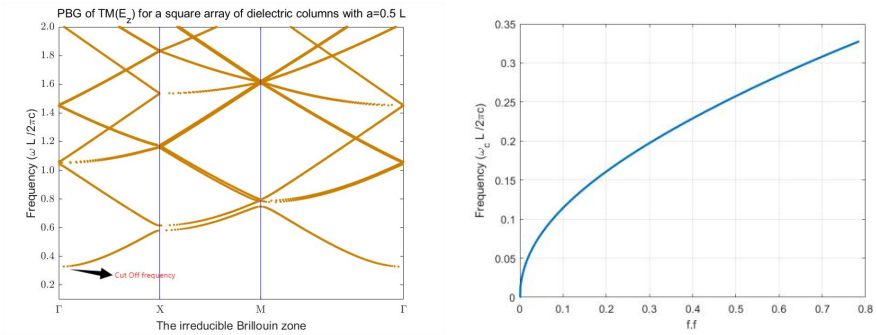

Fig. 2 Band-gap structure(left) and cutoff frequency(right) of photonic crystal(Nb)

Second, we study a 2D square-periodic YBCO superconducting photonic crystal (air background) using DtN. Parameters from Ref. [17]: T_c =92K, λ_0 =200 nm, T=22K, L=2625nm, a=0.18L. Fig. 3(left) displays the band structure; Fig. 3(right) shows bandgap width variations with cylinder radius(f), calculated via DtN.

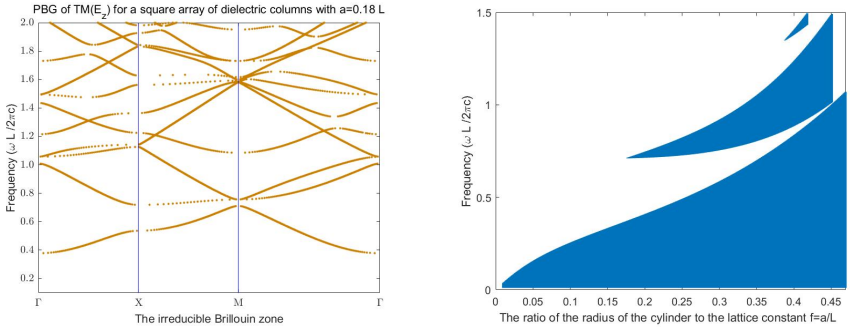

Fig. 3 Band-gap structure of superconducting photonic crystal(YBCO)

3.2 Effect of temperature

Using DtN, we analyze temperature effects in a 2D square-lattice YBCO superconducting photonic crystal (air background, parameters from previous section). Fig.4 shows temperature-dependent curves of low-frequency cutoff and bandgap width, revealing their nonlinear evolution below T_c.

Based on Fig. 4, it has been observed that when the temperature is lower than T_c, the band gap width exhibits a remarkable nonlinear characteristic with respect to the temperature variation.The width of the photonic band gap increases with decreasing temperature, and the cutoff frequency also gradually increases with decreasing temperature. As the critical temperature is approached, both the band gap width and the cutoff frequency change relatively rapidly with temperature. At lower temperatures, however, both the band gap width and the cutoff frequency remain nearly unchanged and tend to level off.This is also consistent with the conclusion of Zhang et al. in the literature [22]. Specifically, for the superconducting photonic crystal given by us, around T_c = 92K (approximately

within the range of 60K - 92K), the variation rates of the bandgap width and the cutoff frequency are relatively high. However, in the low-temperature range (T < 60K), the evolution of the band gap tends to stabilize, and the temperature sensitivity coefficient of the low-frequency cutoff frequency tends to flatten or even remain invariant.

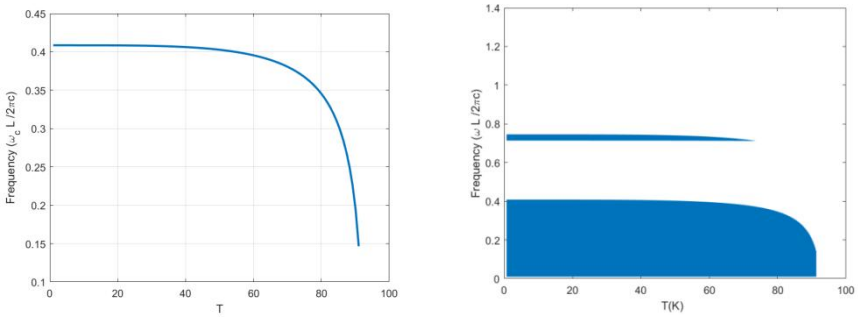

Fig. 4 Effect of temperature on cutoff frequency(left) and bandgap width(right)

4. Summary

Extending the mathematical framework of Dirichlet-to-Neumann mapping, this research resolves photonic bandgaps in 2D superconducting crystal architectures. Unlike conventional plane wave or finite element approaches, the DtN method discretizes only unit boundaries to construct a simplified mapping matrix, reducing the problem to low-complexity eigenvalue calculations, thereby boosting computational efficiency and parameter optimization. We specifically analyze how temperature affects bandgap width and low-frequency cutoff below YBCO's critical temperature, focusing on cylindrical superconducting arrays. Non-cylindrical and 3D SPCs remain beyond this work's scope.

Acknowledgment

The National Natural Science Foundation of China (Grant No. 12171052) and Beijing Natural Science Foundation (Grant No. Z220004) partially funded this research.

References

[1] Yablonovitch E. Inhibited spontaneous emission in solid-state physics and electronics[J]. Physical review letters, 1987, 58(20): 2059.

[2] John S. Strong localization of photons in certain disordered dielectric superlattices[J]. Physical review letters, 1987, 58(23): 2486.

[3] Ma M, Chen K, Bi R, et al. Low loss and wide-band photonic crystal waveguide bend with an open resonator[J]. Optics Communications, 2025: 131904.

[4] Ogusu K, Takayama K. Transmission characteristics of photonic crystal waveguides with stubs and their application to optical filters[J]. Optics letters, 2007, 32(15): 2185-2187.

[5] Sheng G, She K, Shan Z, et al. Ultrahigh-Quality-Factor Topological Photonic Crystal Refractive Index Sensor Based on Second-Order Corner State[J]. IEEE Sensors Journal, 2024.

[6] Chen G, Yao J, Zhu H, et al. Design of a four-channel demultiplexer based on photonic crystals with an ultra-high quality factor[J]. Applied Optics, 2025, 64(10): 2581-2585.

[7] Lozovik Y E, Éĭderman S L. Band structure of superconducting photonic crystals[J]. Physics of the Solid State, 2008, 50: 2024-2027.

[8] Wu C J, Liu C L, Yang T J. Investigation of photonic band structure in a one-dimensional superconducting photonic crystal[J]. Journal of the Optical Society of America B, 2009, 26(11): 2089-2094.

[9] Liu G, Li Y, Jia B, et al. A 3-5 μm broadband YBCO high-temperature superconducting photonic crystal[J]. Chinese Physics B, 2023, 32(3): 034213.

[10] Figotin A, Godin Y A. The computation of spectra of some 2D photonic crystals[J]. Journal of computational physics, 1997, 136(2): 585-598.

[11] Dobson D C. An efficient method for band structure calculations in 2D photonic crystals[J]. Journal of Computational Physics, 1999, 149(2): 363-376.

[12] Xiao W, Gong B, Sun J, et al. Finite element calculation of photonic band structures for frequency dependent materials[J]. Journal of Scientific Computing, 2021, 87: 1-16.

[13] Qiu M, He S. A nonorthogonal finite-difference time-domain method for computing the band structure of a two-dimensional photonic crystal with dielectric and metallic inclusions[J]. Journal of applied physics, 2000, 87(12): 8268-8275.

[14] Liu G, Lu S, Gao Y, et al. Band structure optimization of superconducting photonic crystals based on transmission spectrum calculation[J]. Optics Express, 2023, 31(25): 41905-41918.

[15] Aly A H, Elsayed H A, El-Naggar S A. The properties of cutoff frequency in two-dimensional superconductor photonic crystals[J]. Journal of Modern Optics, 2014, 61(13): 1064-1068.

[16] Wu C J, Wang Z H, Yang T J. Angle-and thickness-dependent photonic band structure in a superconducting photonic crystal[J]. Journal of superconductivity and novel magnetism, 2010, 23: 1395-1399.

[17] LI Y H. Numerical study on enhanced photon localization in yttrium-barium-copper-oxide superconducting network materials [D]. Beijing: Beijing University of Posts and Telecommunications, 2023.

[18] Yuan J, Lu Y Y. Photonic bandgap calculations with Dirichlet-to-Neumann maps[J]. Journal of the Optical Society of America A, 2006, 23(12): 3217-3222.

[19] Yuan J, Lu Y Y. Computing photonic band structures by Dirichlet-to-Neumann maps: The triangular lattice[J]. Optics communications, 2007, 273(1): 114-120.

[20] Hu Z, Lu Y Y. Efficient analysis of photonic crystal devices by Dirichlet-to-Neumann maps[J]. Optics express, 2008, 16(22): 17383-17399.

[21] Tinkham M. Introduction to superconductivity[M]. Courier Corporation, 2004.

[22] Zhang C, Zheng R, Liu Q, Dai H. The Influence of Temperature on the Band Structures in Two dimensional Superconducting Photonic Crystals[J]. Acta Photonica Sinica, 2010, 39(11): 1943